

具有类 CsCl 拓扑的Co^{II}配位聚合物的合成,结构与磁性

林健斌 陈小明*

(中山大学化学与化学工程学院/教育部生物无机与合成化学重点实验室,广州 510275)

摘要: 本工作在溶剂热条件下合成了 2 例以二核或三核 Co^{II}为节点,具有八连接类 CsCl 拓扑的配位聚合物:[Co(na)(ina)]和 [Co₃(na)₄(1,4-chdc)](Hna=nicotinic acid, Hina=isonicotinic acid, 1,4-H₂chdc=cyclohexane-1,4-dicarboxylic acid)。磁性研究表明,2 个配合物均呈现反铁磁行为。

关键词: CsCl; 拓扑结构; 反铁磁

中图分类号: O614.81²

文献标识码: A

文章编号: 100-4861(2008)08-1300-05

Syntheses, Structures and Magnetic Properties of Two Co^{II} Polymers with CsCl-like Topology

LIN Jian-Bin CHEN Xiao-Ming*

(MOE Laboratory of Bioinorganic and Synthetic Chemistry, School of Chemistry and Chemical Engineering, Sun Yat-Sen University, Guangzhou 510275)

Abstract: Two three-dimensional coordination polymers, namely [Co(na)(ina)] (**1**) and [Co₃(na)₄(1,4-chdc)] (**2**) (Hna=nicotinic acid, Hina=isonicotinic acid, 1,4-H₂chdc=cyclohexane-1,4-dicarboxylic acid), with 8-connected CsCl-like topology, have been solvothermally synthesized. The temperature-dependent magnetic susceptibilities were also determined, showing antiferromagnetism in both compounds. CCDC: 688479, **1**; 688480, **2**.

Key words: CsCl; topology; antiferromagnet

The design and synthesis of coordination polymers with three-dimensional (3D) frameworks featuring interesting topologies have been the focus of intense research activity in recent years^[1-5]. The major structural types found in coordination polymers are low-connected topologies in which d-block metal ions are used as nodes for three-, four-, or six-connected^[1,3-6]. The local connectivity numbers larger than six in coordination polymers are rare because of the low coordination sites of d-block metal ions and the sterically demanding nature of organic ligands^[7]. Generally, there

are two ways for constructing highly connected coordination polymers. One is employing *f*-block metal ions centers to construct seven- and eight-connected coordination polymers^[8,9]. The other is based on metal clusters, which is effective to overcome the low coordination numbers of *d*-block metal ions and steric hindrance^[10-12]. Herein, we report two new 3D coordination polymers, namely [Co(na)(ina)] (**1**) and [Co₃(na)₄(1,4-chdc)] (**2**) (Hna=nicotinic acid, Hina=isonicotinic acid, 1,4-H₂chdc=cyclohexane-1,4-dicarboxylic acid), which show 8-connected CsCl-like topology with Co₂ or Co₃

收稿日期:2008-05-19。收修改稿日期:2008-06-23。

“973 计划”(No.2007CB815302)和广东省科技厅(No.04205405)的资助。

*通讯联系人。E-mail:cxm@mail.sysu.edu.cn

第一作者:林健斌,男,25岁,硕士研究生;研究方向:配位化学。

clusters acting as eight-connected nodes, respectively.

1 Experimental

1.1 Reagents and physical measurements

Commercially available reagents were used as received without further purification. Elemental analyses (C, H, N) were performed on a Vario EL elemental analyzer. The FTIR (KBr pellet) spectra were recorded from KBr pellets in the range of 400~4 000 cm⁻¹ on a Bruker TENSOR 27 FTIR spectrometer. X-ray powder diffraction (XRPD) patterns were measured at a Rigaku D/M-2200T automated diffractometer. Magnetic susceptibility measurements of **1** and **2** were performed on a poly-crystalline sample fixed with GE7031 varnish on a Quantum Design MPMS-XL7 SQUID. Data were corrected for the diamagnetic contribution calculated from Pascal constants.

1.2 Synthesis of [Co(na)(ina)] (**1**)

A DMF solution (7 mL) containing CoCl₂·6H₂O (0.238 g, 1 mmol), isonicotinic acid (0.123 g, 1 mmol) and nicotinic acid (0.123 g, 1 mmol) was placed in a Parr Teflon-lined stainless-steel bomb (15 mL), which was sealed and placed in a programmable furnace. The temperature was raised to 160 °C and held at that temperature for 72 h, then cooled to room temperature at 5 °C·h⁻¹. The resulting light blue crystals were collected (0.04 g, *ca.* 13.2% yield based on Co). Anal. calcd (%) for C₁₂H₈CoN₂O₄: C 47.55; H 2.66; N 9.24. Found(%): C 47.18; H 2.87; N 9.34. IR(cm⁻¹): 3 436.4 w, 3 062.8w, 1 627.8vs, 1 544.9s, 1 421.5vs, 1 200.9w,

1 047.0w, 858.3m, 765.7m, 700.1s, 565.9w, 443.6m.

1.3 Synthesis of [Co₃(na)₄(1,4-chdc)] (**2**)

A DMF solution (6 mL) containing CoCl₂·6H₂O (0.238 g, 1 mmol), nicotinic acid (0.123 g, 1 mmol) and 1,4-H₂chdc (0.172 g, 1 mmol) was placed in a Parr Teflon-lined stainless-steel bomb (15 mL), which was sealed and placed in a programmable furnace. The temperature was raised to 170 °C and held at that temperature for 72 h, then cooled to room temperature at 5 °C·h⁻¹. The resulting deep blue crystals were collected (0.02 g, *ca.* 6.6% yield based on Co). Anal. calcd (%) for C₃₂H₂₆Co₃N₄O₁₂: C 46.01; H 3.14; N 6.71. Found(%): C 45.94; H 3.25; N 6.81. IR (cm⁻¹): 3 449.3w, 2 920.0w, 1 616.3vs, 1 570.0vs, 1 523.7s, 1 394.5vs, 1 284.5w, 1 195.8m, 1 043.4m, 1 101.5w, 858.3w, 756.1 m, 702.1m, 569.1w, 447.5m.

1.4 Crystal structure determination

Diffraction intensities were collected on a Bruker Apex CCD area-detector diffractometer (Mo Kα). Absorption corrections were applied by using multi-scan program SADABS^[13]. The structures were solved with direct methods and refined with a full-matrix least-squares technique with the SHELXTL program package^[14]. Anisotropic thermal parameters were applied to all the non-H atoms. The organic H atoms were generated geometrically. Crystal data as well as details of data collection and refinements for the complexes are summarized in Table 1.

CCDC: 688479, **1**; 688480, **2**.

Table 1 Crystallographic data for complexes **1** and **2**

Complex	1	2
Formula	C ₁₂ H ₈ CoN ₂ O ₄	C ₃₂ H ₂₆ Co ₃ N ₄ O ₁₂
Formula weight	303.13	835.37
Crystal system	Monoclinic	Monoclinic
Space group	<i>P</i> 2 ₁ / <i>c</i> (No.14)	<i>C</i> 2/ <i>c</i> (No.15)
<i>a</i> / nm	0.975 1(2)	2.292 4(3)
<i>b</i> / nm	1.171 1(3)	1.039 37(15)
<i>c</i> / nm	1.148 1(3)	1.353 2(2)
<i>β</i> / (°)	112.694(4)	105.250(2)
<i>V</i> / nm ³	1.209 6(5)	3.110 7(8)
<i>Z</i>	4	4
<i>D_c</i> / (g·cm ⁻³)	1.665	1.784

Continued Table 1

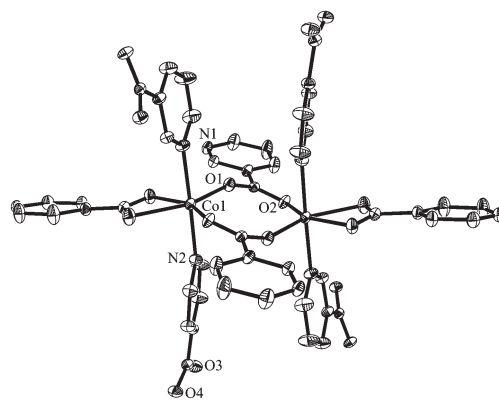
$\mu(\text{Mo } K\alpha) / \text{mm}^{-1}$	1.429	1.657
Reflections collected	5 042	7 130
Unique reflns / R_{int}	2 369 / 0.023 2	2 711 / 0.042 4
$R_1, wR_2 [I > 2\sigma(I)]$	0.036 1, 0.093 1	0.086 2, 0.250 4
R_1, wR_2 (all data)	0.042 1, 0.095 9	0.101 0, 0.264 7
GOF	1.046	1.036
$\Delta\rho_{\text{min/max}} / (\text{e} \cdot \text{nm}^{-3})$	766 / -440	1 021 / -1 868

$$R_1 = \sum \|F_o\| - \|F_c\| / \sum \|F_o\|, wR_2 = [\sum w(\|F_o\| - \|F_c\|)^2 / \sum w\|F_o\|^2]^{1/2}.$$

2 Results and discussion

2.1 Crystal structure of 1

The crystal structure of **1** is shown in Fig.1. Selected bond lengths and angles are given in Table 2. Each Co^{II} ion is coordinated to three na and two ina ligands in a distorted octahedral N_2O_4 geometry (Co-N/O 0.199 9(2)~0.223 0(2) nm). Each na ligand acts as a μ_3 -ligand with its carboxylate group bridging two Co^{II} ions that are separated by 0.411 9 nm. Each ina ligand acts as a μ_2 -ligand with its carboxylate group chelating a Co^{II} ion. In other words, each dinuclear Co^{II} cluster

Fig.1 Dinuclear Co^{II} structure of complex **1**Table 2 Selected bond lengths (nm) and angles ($^\circ$) of complexes **1** and **2**

Complex 1					
Co(1)-O(1)	0.199 9(2)	Co(1)-O(4B)	0.213 2(2)	Co(1)-N(1C)	0.216 9(2)
Co(1)-O(2A)	0.202 0(2)	Co(1)-N(2)	0.215 6(2)	Co(1)-O(3B)	0.223 0(2)
O(1)-Co(1)-O(2A)	115.63(8)	O(4B)-Co(1)-N(2)	86.18(9)	O(1)-Co(1)-O(3B)	150.66(8)
O(1)-Co(1)-O(4B)	90.81(8)	O(1)-Co(1)-N(1C)	87.65(8)	O(2A)-Co(1)-O(3B)	93.58(7)
O(2A)-Co(1)-O(4B)	153.56(8)	O(2A)-Co(1)-N(1C)	89.45(8)	O(4B)-Co(1)-O(3B)	60.01(7)
O(1)-Co(1)-N(2)	92.49(9)	O(4B)-Co(1)-N(1C)	91.79(9)	N(2)-Co(1)-O(3B)	88.74(9)
O(2A)-Co(1)-N(2)	92.32(8)	N(2)-Co(1)-N(1C)	177.97(9)	N(1C)-Co(1)-O(3B)	90.15(9)
Complex 2					
Co(1)-O(6)	0.207 5(5)	Co(2)-O(3)	0.199 6(5)	Co(2)-N(1D)	0.208 5(7)
Co(1)-O(4)	0.215 1(5)	Co(2)-O(2)	0.205 7(7)	Co(2)-O(1)	0.231 5(7)
Co(1)-N(2B)	0.215 9(6)	Co(2)-O(5)	0.206 0(6)	Co(2)-O(6)	0.233 7(6)
O(6)-Co(1)-O(6A)	91.8(3)	O(3)-Co(2)-O(2)	102.8(3)	O(5)-Co(2)-O(1)	83.2(2)
O(6)-Co(1)-O(4A)	91.7(2)	O(3)-Co(2)-O(5)	113.0(2)	N(1D)-Co(2)-O(1)	91.8(2)
O(6)-Co(1)-O(4)	92.8(2)	O(2)-Co(2)-O(5)	137.8(2)	O(3)-Co(2)-O(6)	97.8(2)
O(4A)-Co(1)-O(4)	173.5(3)	O(3)-Co(2)-N(1D)	95.2(2)	O(2)-Co(2)-O(6)	95.8(2)
O(6)-Co(1)-N(2B)	88.2(2)	O(2)-Co(2)-N(1D)	103.9(3)	O(5)-Co(2)-O(6)	58.9(2)
O(6)-Co(1)-N(2C)	179.9(3)	O(5)-Co(2)-N(1D)	94.6(3)	N(1D)-Co(2)-O(6)	153.3(2)
O(4)-Co(1)-N(2C)	87.3(2)	O(3)-Co(2)-O(1)	161.6(2)		
N(2B)-Co(1)-N(2C)	91.9(3)	O(2)-Co(2)-O(1)	58.9(2)		

Symmetry codes for **1**: A: $-1-x, -y, -1-z$; B: $-x, 0.5+y, -0.5-z$; C: $x, 0.5-y, -0.5+z$; for **2**: A: $-x, y, 0.5-z$; B: $x, 1-y, -0.5+z$; C: $-x, 1-y, 1-z$; D: $0.5-x, 0.5+y, 0.5-z$.

binds simultaneously to four na and four ina ligands. By treating the dinuclear cluster as a single node and the ligand as linker, a CsCl-like^[15] 3D network sustained by 8-connected nodes is formed, as illustrated in Fig.2.

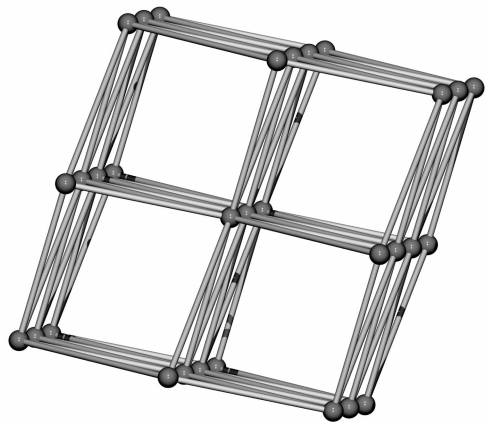


Fig.2 CsCl-like net

2.2 Crystal structure of 2

The crystal structure of **2** is shown in Fig.3 (a). Selected bond lengths and angles are given in Table 2. Two Co^{II} ions are crystallographically unique, and both have distorted octahedral environments. Co(1) is located at a twofold axis, and coordinated to four na and two

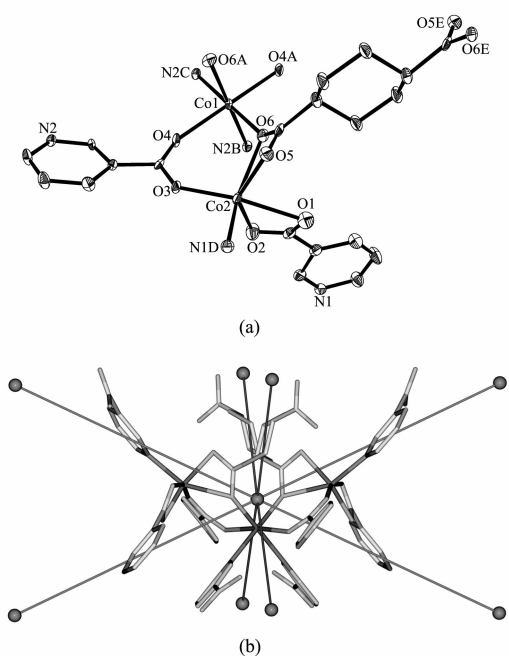


Fig.3 (a) Coordination environments in **2** (symmetry codes: A: $-x, y, 0.5-z$; B: $x, 1-y, -0.5+z$; C: $-x, 1-y, 1-z$; D: $0.5-x, 0.5+y, 0.5-z$; E: $-x+1/2, y-1/2, -z+1/2$); (b) view of the 8-connected trinuclear cluster connected to eight neighbors in **2**

1,4-chdc ligands in a distorted octahedral N_2O_4 geometry (Co-N/O 0.207 5(5)~0.215 9(6) nm). Co(2) is coordinated to three na and one 1,4-chdc ligands in a distorted octahedral NO_5 geometry (Co-N/O 0.199 6(5)~0.233 7(6) nm). One na acts as a μ_3 -ligand with its carboxylate group bridging two Co^{II} ions that are separated by 0.383 1 nm, the other acts as a μ_2 -ligand with its carboxylate group chelating a Co atom. Each 1,4-chdc acts as a μ_4 -ligand with each carboxylate group connects two Co^{II} ions with the $\mu_2\text{-}\eta^1\text{:}\eta^2$ mode. In other words, each trinuclear Co^{II} cluster binds to eight na ligands and two 1,4-chdc ligands simultaneously. By treating the trinuclear as a single node, the 8-connected node connects to eight neighbors through these ten ligands (Fig.3(b)), forming a CsCl-like 3D network similar to complex **1**, as illustrated in Fig.2.

2.3 Magnetic properties

The phase purities of **1** and **2** used for magnetic measurement have been confirmed by XRPD (Fig.4). The variable-temperature magnetic susceptibilities of **1** and **2** were measured in the temperature range from 300 to 2 K (Fig.5), at a magnetic field strength of 1 000 Oe.

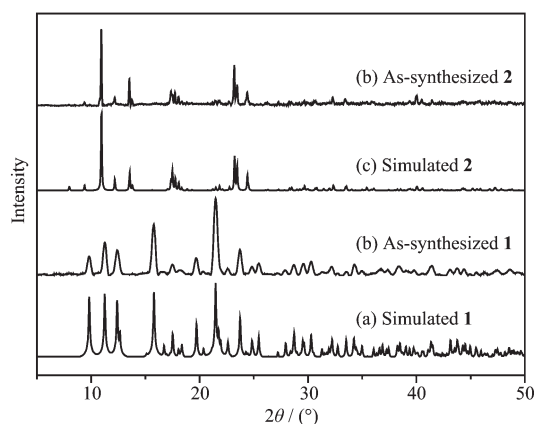


Fig.4 XRPD patterns of **1** and **2**

For **1**, the $\chi_m T$ value at room temperature is *ca.* $5.23 \text{ cm}^3 \cdot \text{mol}^{-1} \cdot \text{K}$, higher than the spin-only value of $3.75 \text{ cm}^3 \cdot \text{mol}^{-1} \cdot \text{K}$ expected for two noncoupled Co^{II} ions with $g=2.0$, owing to a significant orbital contribution of a high-spin octahedral Co^{II} . The $\chi_m T$ product decreases with decreasing temperature, which is a typical behavior of the antiferromagnetically coupled magnetic pair. The magnetic susceptibility in the range of 300~50 K can be well fitted by the Curie-Weiss law

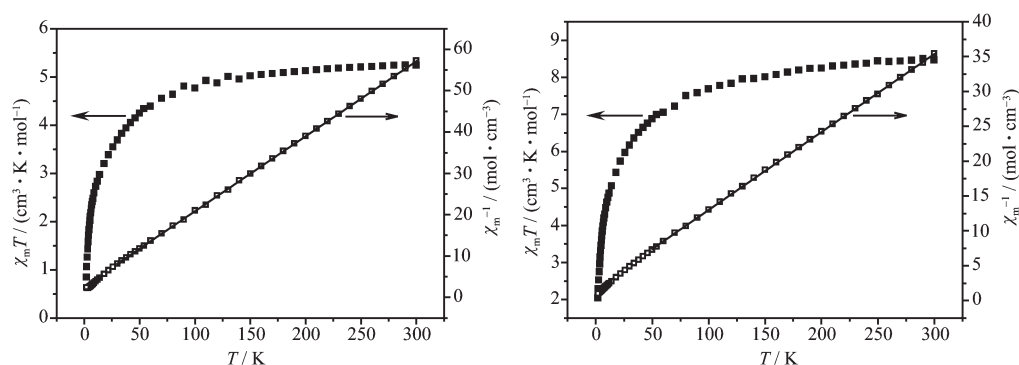


Fig.5 $\chi_m T$ - T and χ_m^{-1} - T for **1** (left) and **2** (right) from 300 to 2 K at 1000 Oe

with a Curie constant $C=5.51 \text{ cm}^3 \cdot \text{mol}^{-1} \cdot \text{K}$ and a Weiss constant θ of -14.6 K , which is a further indication of the weak antiferromagnetic interactions in **1**.

For **2**, the $\chi_m T$ value at room temperature is *ca.* $8.45 \text{ cm}^3 \cdot \text{mol}^{-1} \cdot \text{K}$, higher than the spin-only value of $5.625 \text{ cm}^3 \cdot \text{mol}^{-1} \cdot \text{K}$ expected for three noncoupled Co^{II} ions with $g=2.0$, owing to a significant orbital contribution of a high-spin octahedral Co^{II} . The $\chi_m T$ product decreases with decreasing temperature, which is a typical behavior of the antiferromagnetically coupled magnetic pair. The magnetic susceptibility in the range of $300 \sim 50 \text{ K}$ obeys the Curie-Weiss law with a Curie constant $C=8.94 \text{ cm}^3 \cdot \text{mol}^{-1} \cdot \text{K}$ and a Weiss constant θ of -16.3 K in **2**. The absolute values of Weiss constant θ of **2** is larger than **1**. According to the crystal structures, the single bridging oxygen can be assumed that the superexchange interactions between Co^{II} ions of **2** is stronger than **1**.

References:

- [1] Batten S R, Robson R. *Angew. Chem. Int. Ed.*, **1998**, *37*:1461~1494
- [2] Robson R. *J. Chem. Soc., Dalton Trans.*, **2000**:3735~3744
- [3] Carlucci L, Ciani G, Proserpio D M. *Coord. Chem. Rev.*, **2003**, *246*:247~289
- [4] Zhang J P, Lin Y Y, Zhang W X, et al. *J. Am. Chem. Soc.*, **2005**, *127*:14162~14163
- [5] Halper S R, Do L, Stork J R, et al. *J. Am. Chem. Soc.*, **2006**, *128*:15255~15268
- [6] Ferey G, Mellot-Draznieks C, Serre C, et al. *Acc. Chem. Res.*, **2005**, *38*:217~225
- [7] Zhang X M, Zheng Y Z, Li C R, et al. *Cryst. Growth Des.*, **2007**, *7*:980~983
- [8] Long D L, Blake A J, Champness N R, et al. *Angew. Chem. Int. Ed.*, **2001**, *40*:2444~2447
- [9] Long D L, Hill R J, Blake A J, et al. *Angew. Chem. Int. Ed.*, **2004**, *43*:1851~1854
- [10] Li D, Xiao P, Zhou R, et al. *Angew. Chem. Int. Ed.*, **2005**, *44*:4175~4178
- [11] Zhang X M, Fang R Q, Wu H S. *J. Am. Chem. Soc.*, **2005**, *127*:7670~7671
- [12] Cairns A J, Perman J A, Wojtas L, et al. *J. Am. Chem. Soc.*, **2008**, *130*:1560~1561
- [13] Sheldrick G M. *SADABS 2.05*. University Göttingen, Germany
- [14] *SHELXTL 6.10*. Bruker Analytical Instrumentation: Madison, Wisconsin, USA, **2000**.
- [15] Zhang M, Kang Y, Zhang J, et al. *Eur. J. Inorg. Chem.*, **2006**:2253~2258